

# 1 Convolutional Neural Network Measurement of 2 Non-Fiducial Cosmic Ray Electrons with the DAMPE 3 Experiment

---

4 **Enzo Putti-Garcia,<sup>a,\*</sup> Andrii Tykhonov,<sup>a</sup> David Droz<sup>a</sup> and Xin Wu<sup>a</sup> for the DAMPE**  
5 **collaboration**

6 <sup>a</sup>*University of Geneva*

7 *E-mail:* [enzo.putti-garcia@unige.ch](mailto:enzo.putti-garcia@unige.ch)

8 The Dark Matter Particle Explorer (DAMPE) is a space-based Cosmic Ray (CR) observatory with the aim, among others, to study Cosmic Ray Electrons (CREs) up to 10 TeV. Due to the low CRE rate at multi-TeV range, we aim at increasing the acceptance by selecting events outside the fiducial volume. The complex topology of non-fiducial events require special treatment with sophisticated analysis tools. Therefore, we propose a Convolutional Neural Network (CNN) to identify non-fiducial CREs and reject background events, based on their interaction in DAMPE's calorimeter. In the following, we will present the aforementioned method in order to precisely identify such events.

38th International Cosmic Ray Conference (ICRC2023)  
26 July - 3 August, 2023  
Nagoya, Japan



---

\*Speaker

## 1. Introduction

The Dark Matter Particle Explorer (DAMPE) is a Cosmic Ray (CR) and Gamma-ray experiment in operation since December 2015 [1]. DAMPE aims, among others, to study Cosmic Ray Electrons (CREs) up to 10 TeV. It is composed of 4 sub-detectors, namely a Plastic Scintillator Detector, a Silicon-tungsten TracKer-converter, a Bismuth Germanium Oxide (BGO) calorimeter [2] and a NeUtron Detector. The sub-detectors mentioned above ensure the precise identification of impinging CRs, while providing an accurate measurement of their absolute charge, energy and direction.

Due to their light mass, CREs experience energy losses as they propagate, due to processes like synchrotron radiation and inverse Compton scattering. Consequently, it is anticipated that electrons at energies higher than a few TeV originate from nearby sources, i.e. within a distance of 1 kiloparsec (kpc) [3] or times older than  $\sim 10^5$  years [4]. In addition, the aforementioned losses lead to a steeper energy spectrum which, combined to the already lower CRE flux with respect to other species, make them relatively rare at high energies. Moreover, several dark matter models predict positron emission as a result of annihilation or decay [5], which could then be seen as e.g. an excess in the high energy CRE spectrum. In 2017, DAMPE published its first measurement of the CRE flux using 1.5 years of data and featuring the direct detection of a break at 0.9 TeV [6]. While impactful, this results was limited to 5 TeV due indeed to low CRE flux (only 11 events were detected between 3 and 5 TeV). In order to enhance and expand our current understanding in the multi-TeV range, it is essential to improve the accuracy and increase the statistics. Hence, we enlarge the acceptance by selecting events outside of the fiducial volume, which are typically events with a large incidence angle (see Section 2). However, those events carry a complex topology. In [6], the authors develop an analytical classifier ( $\zeta$ ) for proton/electron discrimination, which is based on the topology of the particle shower in the calorimeter. The  $\zeta$  variable has however lower efficiency at higher energies. Additionally, non-fiducial events with large incidence angle might lead to a particle shower which might not be well contained inside the BGO, thus making it difficult to efficiently identify electrons. As a result, in this paper we propose a Convolutional Neural Network (CNN) for electron/proton outside of DAMPE's fiducial volume. In Section 3, we will introduce 3 CNN models and compare their discrimination power with respect to  $\zeta$ .

## 2. Non-Fiducial Events

To improve and expand the CRE flux measurement at higher energies, it is necessary to increase the available statistics. However, as mentioned previously due to their light mass CREs lose energy combined with a lower flux compared to other CR resulting difficult to extend the flux above a few TeV. Nonetheless, we can accomplish it by including the analysis events outside of the fiducial volume. In order to achieve this, we enhance the acceptance by including non-fiducial events.

The analysis of DAMPE data involves applying a series of cleaning filters, internally known as "skim". These selections are based on the behavior of events observed in the BGO calorimeter. Furthermore they ensure that the events are well reconstructed and contained in the calorimeter:

- rejecting events that enter from the sides.
- rejecting events where the shower direction cannot be reconstructed.

- Ensuring that the reconstructed shower direction extrapolates to the top and bottom of the BGO sensitive volume within a distance of 280 mm from the center, in either the X or Y direction.

These cuts guarantee that the events considered are well reconstructed and contained in the calorimeter.

Non-fiducial events are selected using a similar process, with the exception that we reverse the last cut by selecting events for which their projection of the shower vector is more than 280 mm away from the center in both the X and Y directions.

The analysis chain first involves preselection cuts to reject ions, obvious protons, or poorly reconstructed events in a similar fashion to the 2017 results [6]. Additionally, non-fiducial events often exhibit a complex shower topology in the BGO, requiring more sophisticated techniques to distinguish electrons from protons.

### 3. Classification of electrons using a Convolutional Neural Network

Machine Learning (ML) has become an efficient tool, ranging from data-driven applications, computer vision to speech recognition. Hence, particle physics has also found applications from Monte-Carlo (MC) simulations to data analysis [7]. Successful deep learning techniques used in DAMPE for electron/positron discrimination have already been developed [8, 9] as well as tracking reconstruction [10]. Hence, we decided to use a pattern recognition method, known as CNN [11], for which the input will be an image of the deposited energy in the calorimeter [12]. The BGO is composed of 14 layers in a hodoscopic arrangement with each layer comprising of 22 BGO bars. We combined both directions to construct the input image, the size of which amounts to  $14 \times 22$  pixels (Figure 1). This representation of a particle shower is certainly unphysical, that said, the development of the shower in the calorimeter is dependent on how the particle interacts in the different layers which results in a correlation between the different levels of BGO. For this reason given separated images will result in a lack of information for the CNN and as consequence a lower discrimination power.

The CNN structure is shown in Figure 2. As described in [8], to avoid a compression of the CNN output into a finite range, we decided, after training the network, to remove the sigmoid function from the CNN's output layer. For the training we used the same number (800 thousand events) of simulated proton and electron events, such that we have an equal representation of both species at all energies. Finally for the training, simulated data was split into a 70/30 ratio for training/validation of the CNN model. The CNNs were trained using Tensorflow [13], using using Nvidia GPUs. They were trained during 100 iterations (epochs) with the Adam optimiser [14].

#### 3.1 Results

We trained 3 different CNNs, to investigate in parallel the effect of different cleaning cuts. Specially, the CNNs used in this work can be classified as: v0, v0c and v1c. All three have the exact same architecture (Figure 2). Model v0c differs from the baseline model, v0, by the addition of a very loose cut  $\zeta < 100 \text{ mm}^4$  that allows the removal of clear proton events. Model v1c further

---

<sup>1</sup>This cut is 100% efficient on electrons

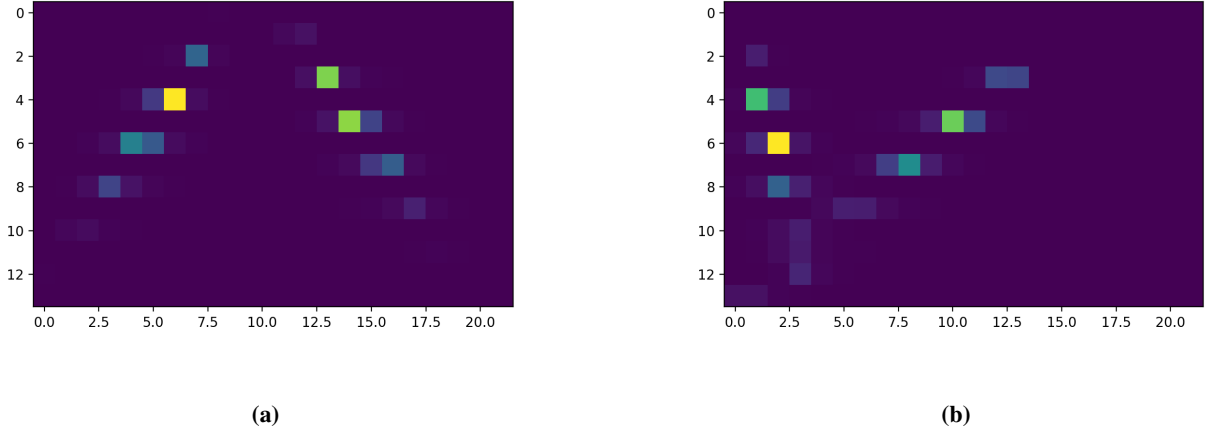


**Figure 1:** Example of input images for the CNN, for which we combined the X and Y views into one image. Figure (a): Image of a simulated electron, with kinetic energy of 17.74 TeV. Figure (b): Image of a simulated proton, with kinetic energy of 12.99 TeV. Each pixel represents the energy deposited in one of the BGO bars in the calorimeter. Linear colour scale

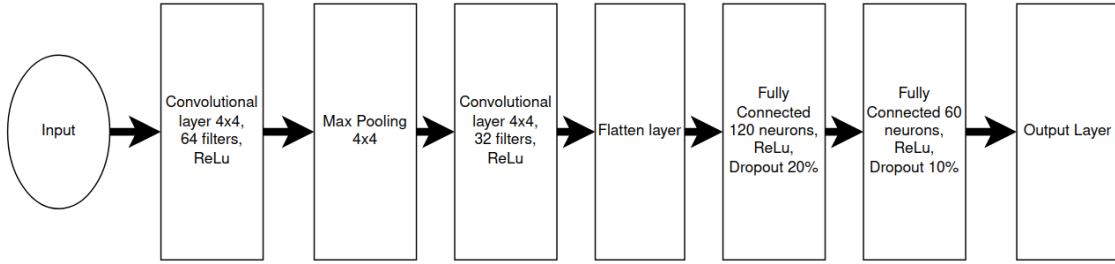


**Figure 2:** Architecture of the CNN used for electron/proton discrimination. Note the absence of activation function at the output layer, see text for details.

86 adds a cut to remove events with large incidence angle.

87 To verify that the CNN is able to classify electrons and protons, the distribution of  $v_0$  model is  
88 shown as a function of energy (as seen in Figure 3), whereas both  $v_0c$  and  $v_1c$  have similar shapes  
89 therefore are not shown.

90 A good separation between protons and electrons is evident at all energies while maintaining  
91 stable distribution shapes. Despite the good separation between background and signal distributions,  
92 there is clear contamination contribution from protons into the electron region. Since some events  
93 have similar shape in BGO (for protons/electrons), it is expected that the CNN will attribute them  
94 similar output values. In order to quantify the efficiency of the CNN and compare with the classical  
95 method,  $\zeta$ , we decided to plot the Receiver Operating Characteristic (ROC) curve, as seen in Figure  
96 4a. For an electron efficiency of 90%, the 3 models resulted in a background contamination of  
97  $\approx 0.9 \cdot 10^{-3}$  while the analytical method resulted in  $\approx 10^{-2}$ , thus improving the separation power  
98 by a factor 10.

99 To better quantify the dependence of the performances on energy, we decided to select the

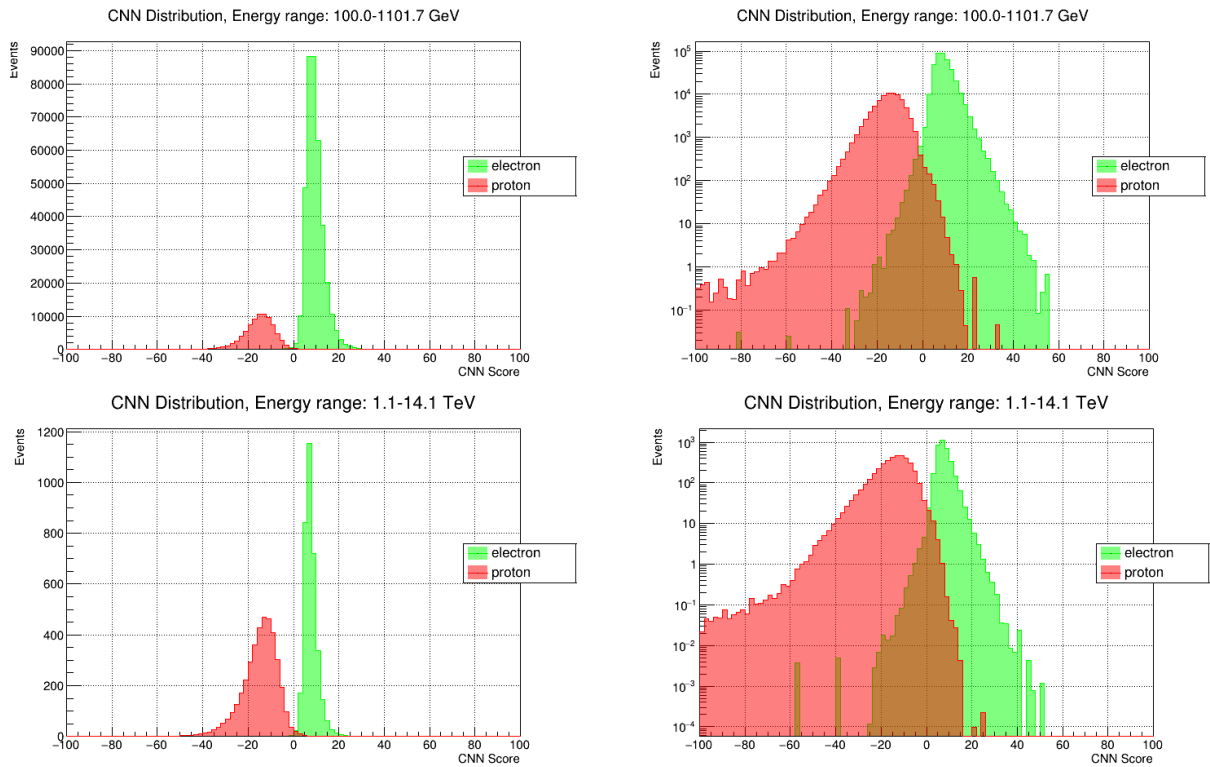


**Figure 3:** Distribution of  $v_0$ 's output values for different energy bins. Top: 100- 1102 GeV, bottom: 1.1-14 TeV. Left: linear scale, Right: logarithmic scale.

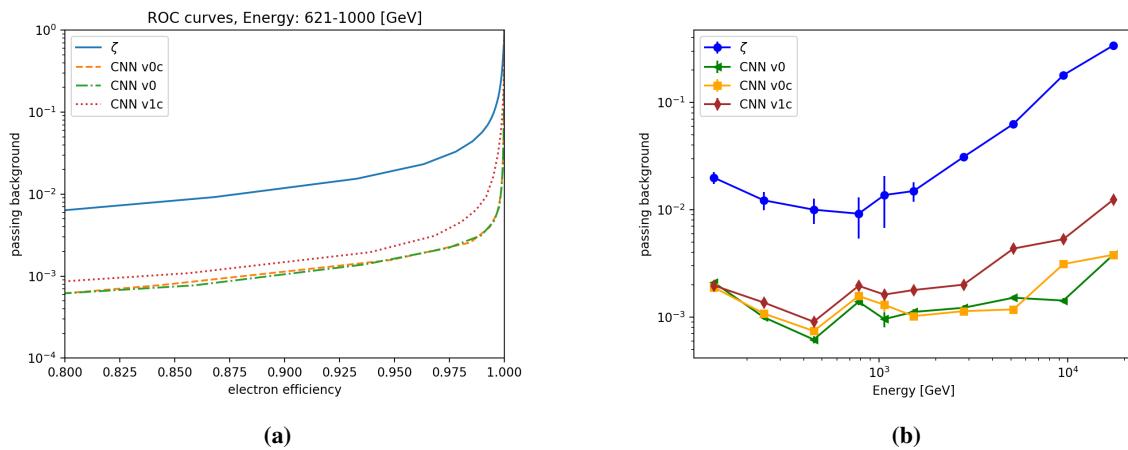


**Figure 4:** Performances of the CNN classifiers versus the classical method  $\zeta$  based on MC. Figure (a): ROC curves on a selected energy range, showing background contamination versus electron efficiency. Figure (b): Background contamination in the signal region at an efficiency of 90%, as function of the energy in the calorimeter.

100 remaining background corresponding to a signal efficiency of 90%, such that we can assess the  
101 CNN and  $\zeta$  efficiency at all energies, as shown in Figure 4b.

102 An improvement of approximately one order of magnitude is evident. The 3 CNN models  
103 show similar behaviour at energies below 1 TeV while models v0 and v0 with  $\zeta < 100 \text{ mm}^4$  cut  
104 show better performances at the TeV scale.

#### 105 4. Conclusion

106 In this work, we presented a CNN model as a tool to separate protons from electrons, on CR  
107 data outside the fiducial volume of DAMPE. We used the deposited energy on the calorimeter and  
108 combined the X-Y directions to build an 14x22 image of a particle's shower in the BGO. We trained 3  
109 CNNs using the images from MC data (protons and electrons) and finally quantify the discrimination  
110 power of the different models and compared to the analytical method of [6]. The main motivation  
111 can be found at multi-TeV energies, where CREs are of prime interest for Astroparticle Physics.  
112 However, the light mass of electrons results in energy loss, while they propagate, due to synchrotron  
113 radiation and inverse Compton scattering, combined to CREs having a lower flux compare to  
114 other CR species. Consequently, at those energies the statistics are scarce. The improvement and  
115 extension of DAMPE's electron-positron flux needs a gain of electrons candidates, which can be  
116 obtained by increasing the acceptance. However this leads to having events with a complex shower  
117 topology. We showed that a CNN can successfully recover these events with a good background  
118 rejection power, improving by a factor 10 upon the analytical method, at all energies.

119 However, the CNNs performances were evaluated only on simulated data only. A final assess-  
120 ment would require evaluating the CNN on real data from our detectors, which is the immediate  
121 next step of the study. Nonetheless this work shows that the discriminatory power of a CNN at all  
122 energies could improve current DAMPE results and help extending the flux.

#### 123 5. Acknowledgements

124 The DAMPE mission was funded by the strategic priority science and technology projects  
125 in space science of Chinese Academy of Sciences (CAS). In China, the data analysis was sup-  
126 ported by the National Key Research and Development Program of China (No. 2022YFF0503302)  
127 and the National Natural Science Foundation of China (Nos. 12220101003, 11921003, 11903084,  
128 12003076 and 12022503), the CAS Project for Young Scientists in Basic Research (No. YSBR061),  
129 the Youth Innovation Promotion Association of CAS, the Young Elite Scientists Sponsorship Pro-  
130 gram by CAST (No. YESS20220197), and the Program for Innovative Talents and Entrepreneur  
131 in Jiangsu. In Europe, the activities and data analysis are supported by the Swiss National Sci-  
132 ence Foundation (SNSF), Switzerland, the National Institute for Nuclear Physics (INFN), Italy, and  
133 the European Research Council (ERC) under the European Union's Horizon 2020 research and  
134 innovation programme (No. 851103).

#### 135 References

- 136 1. Chang, J. *et al.* The DArk Matter Particle Explorer mission. *Astroparticle Physics* **95**, 6–24.  
137 ISSN: 0927-6505 (2017).

- 138 2. Zhang, Z. *et al.* The calibration and electron energy reconstruction of the BGO ECAL of  
139 the DAMPE detector. *Nuclear Instruments and Methods in Physics Research Section A:  
140 Accelerators, Spectrometers, Detectors and Associated Equipment* **836**, 98–104. ISSN: 0168-  
141 9002 (2016).
- 142 3. Evoli, C., Amato, E., Blasi, P. & Aloisio, R. Galactic factories of cosmic-ray electrons and  
143 positrons. *Phys. Rev. D* **103**, 083010 (8 2021).
- 144 4. Kobayashi, T., Komori, Y., Yoshida, K. & Nishimura, J. The Most Likely Sources of High-  
145 Energy Cosmic-Ray Electrons in Supernova Remnants. **601**, 340–351 (2004).
- 146 5. Turner, M. S. & Wilczek, F. Positron line radiation as a signature of particle dark matter in  
147 the halo. *Phys. Rev. D* **42**, 1001–1007 (4 1990).
- 148 6. DAMPE Collaboration. Direct detection of a break in the teraelectronvolt cosmic-ray spectrum  
149 of electrons and positrons. en. *Nature* **552**, 63–66. ISSN: 0028-0836, 1476-4687 (2017).
- 150 7. Albertsson, K. *et al.* Machine Learning in High Energy Physics Community White Paper. *J.  
151 Phys.: Conf. Ser.* **1085**, 022008. ISSN: 1742-6588, 1742-6596 (2018).
- 152 8. Droz, D. *et al.* A neural network classifier for electron identification on the DAMPE experi-  
153 ment. *J. Inst.* **16**, P07036. ISSN: 1748-0221 (2021).
- 154 9. Xu, Z. *et al.* An Unsupervised Machine Learning Method for Electron–Proton Discrimination  
155 of the DAMPE Experiment. *Preprint* **8**, 570 (2022).
- 156 10. Tykhonov, A. *et al.* A deep learning method for the trajectory reconstruction of cosmic rays  
157 with the DAMPE mission. *Astroparticle Physics* **146**, 102795. ISSN: 0927-6505 (2023).
- 158 11. Goodfellow, I., Bengio, Y. & Courville, A. *Deep Learning* [http://www.deeplearningbook.](http://www.deeplearningbook.org)  
159 [org](http://www.deeplearningbook.org) (MIT Press, 2016).
- 160 12. Stolpovskiy, M. *et al.* Machine learning-based method of calorimeter saturation correction  
161 for helium flux analysis with DAMPE experiment. *Journal of Instrumentation* **17**, P06031  
162 (2022).
- 163 13. Martín Abadi *et al.* *TensorFlow: Large-Scale Machine Learning on Heterogeneous Systems*  
164 2015. <https://www.tensorflow.org/>.
- 165 14. Kingma, D. P. & Ba, J. *Adam: A Method for Stochastic Optimization* 2017. arXiv: [1412.6980](https://arxiv.org/abs/1412.6980)  
166 [[cs.LG](https://arxiv.org/abs/1412.6980)].